

NUMERICAL INVESTIGATION AND EXPERIMENTAL VALIDATION OF HEAT TRANSFER IN A SMALL SIZE SHELL AND TUBE HEAT EXCHANGER

Mateo Kirinčić* – Anica Trp – Kristian Lenić

Department of Thermodynamics and Energy Engineering, Faculty of Engineering, University of Rijeka, Vukovarska 58, 51000 Rijeka, Croatia

ARTICLE INFO

Article history:

Received: 30.6.2016.

Received in revised form: 7.11.2016.

Accepted: 8.11.2016.

Keywords:

Heat transfer

Small size shell and tube heat exchanger

Segmental baffles

Finite volume method

Experimental validation

Abstract:

Heat exchangers are integrated in all process and energy plants. Shell and tube heat exchanger designs are most commonly used. The efficiency and performance of the device can be determined both experimentally and numerically. In this study, a numerical model of heat transfer in a small size shell and tube heat exchanger is presented, and the results are compared with experimental data. The problem with laminar flow and steady state heat transfer was solved using the finite volume method. Three experiments were performed, and all of them showed a high match between outlet fluid temperatures. As additional validation, heat flux balance was set and calculated for both methods, which also showed a considerable match. It can be concluded that the model accurately predicts physical phenomena in analyzed heat exchanger, and can be used in further studies.

1 Introduction

Heat exchanger types and designs vary greatly depending on their use, but they all possess a common feature: their purpose is to transfer heat between two fluids so as to heat up or cool down one of them. Of all designs probably the most common is the shell-and-tube one; the heat exchanger consists of a tube bundle and an outer shell surrounding it. One fluid flows through the tubes, and the other around them. In order to support the tube bundle and increase heat transfer by increasing turbulence and retention of one fluid, flow-directing panels called baffles are used. Since experimental research is often complex and financially demanding, it is useful to design a mathematical model for a heat transfer problem in a heat exchanger and easily determine all heat transfer-

related data required, especially when it requires varying sets of inlet parameters.

Previous research has dealt with similar problems, but some was purely experimental or purely numerical, and the research that included both methods has used heat exchangers with different geometry and different kinds of flow. For example, Jadhav and Koli [1] performed some numerical research into pressure drops and heat transfer coefficient variations on the shell side depending on baffle number and height, as well as shell diameter. A similar study performed by Arjun and Gopu [2] dealt with optimization of a numerical model of a heat exchanger with helical baffles, regarding the flow rate and helix angle. Wen et al. [3] proposed a ladder-type fold baffle to enhance the performance of a heat exchanger with helical baffles, which resulted

* Corresponding author. Tel. +38551651517
E-mail address: mateo.kirincic@riteh.hr

in significant improvement in heat transfer coefficient and thermal performance in general.

You et al. [4] presented a numerical validation of a heat exchange problem for a turbulent flow and suggested heat transfer enhancements by structural and geometrical modifications. A research performed by Pal et al. [5] dealt with turbulent heat transfer using the $k-\epsilon$ method in a small size shell and tube heat exchanger, both with or without baffles, observing that the cross flow near the nozzle region has a much higher effect on the heat transfer, as opposed to the parallel region. The correlation between heat exchanger size and nozzle region influence was previously observed by Kim and Aicher [6].

A combined research was performed by Vukić et al. [7] for a turbulent flow using the PHOENICS code. Yang and Liu [8] described a numerical model with experimental validation of a novel heat exchanger with new plate baffles, as opposed to rod baffles, which resulted in an improved performance. Yang et al. [9] designed four different numerical models (the unit model, periodic model, porous model, whole model) of heat transfer in a rod-baffle shell and tube heat exchanger and compared it to experimental data, resulting in fairly good results in all models except the unit one.

The goal of this research is to investigate the validity of a 3D model of a heat transfer problem in a small size shell-and-tube heat exchanger with segmental baffles by comparing the results of a numerical calculation to experimental results acquired from the device. The accuracy is to be determined by three separate experiments, all with different inlet parameters. Primary values that are to be compared are the outlet fluid temperatures and heat fluxes acquired and calculated by both methods. Experiments were performed on the educational *TD360c* heat exchanger, manufactured by TecQuipment Ltd. Both fluids are single phase (liquid water), the flow is laminar and countercurrent, and heat transfer is steady state. The numerical method used is the finite volume method, and the model was designed in ANSYS software.

2 Mathematical model

Mathematical modeling is used to describe an actual physical phenomenon using differential equations, and initial and boundary conditions. Differential equations describe the change of a variable within the

domain, initial conditions define values of all variables in the initial moment, and boundary conditions define the variables at geometric boundaries of the domain.

2.1 Physical problem

The device in which the heat transfer problem takes place is a small size heat exchanger, consisting of:

- outer shell
- 7 4/6 mm tubes in the tube bundle
- 3 segmental baffles
- inlet and outer plena.

Hot water enters through the inlet plenum, flows through the tubes, and exits at the outer plenum. Cold water flows on the shell side around the tubes, entering and exiting the device through the nozzles on the top. Fig. 1 shows dimensions of analyzed heat exchanger.

Since the heat transfer environment, i.e. the device, is longitudinally symmetrical (as shown in Fig. 1) and both fluids feature a single flow, it is sufficient to single out one half of the heat exchanger for an adequate thermodynamic analysis; since the physical changes on that side mirror themselves along the longitudinal symmetry plane, thus avoiding redundant calculation and saving time and memory. Because of that, only the longitudinal half is used as the geometric model environment, and it is displayed in Fig. 2.

2.2 Governing equations

The model domain includes three subdomains; hot water, wall, and cold water, each of them represented in Fig. 3. It is assumed that there is no heat transfer between cold water and shell. For each of the subdomains, the conservation equations will be applied. These include the continuity equation, which presumes that the amount of matter entering a certain volume of space must be equal to the amount exiting it; momentum equations (Navier-Stokes equations), the three equations in three spatial directions defining the balance of forces in a volume; and the energy equation, also called the heat balance equation. It is also assumed that the physical properties of the materials, such as density, heat capacity, conductivity, and viscosity are constant. Since the wall is a solid, only the energy equation applies for this subdomain.

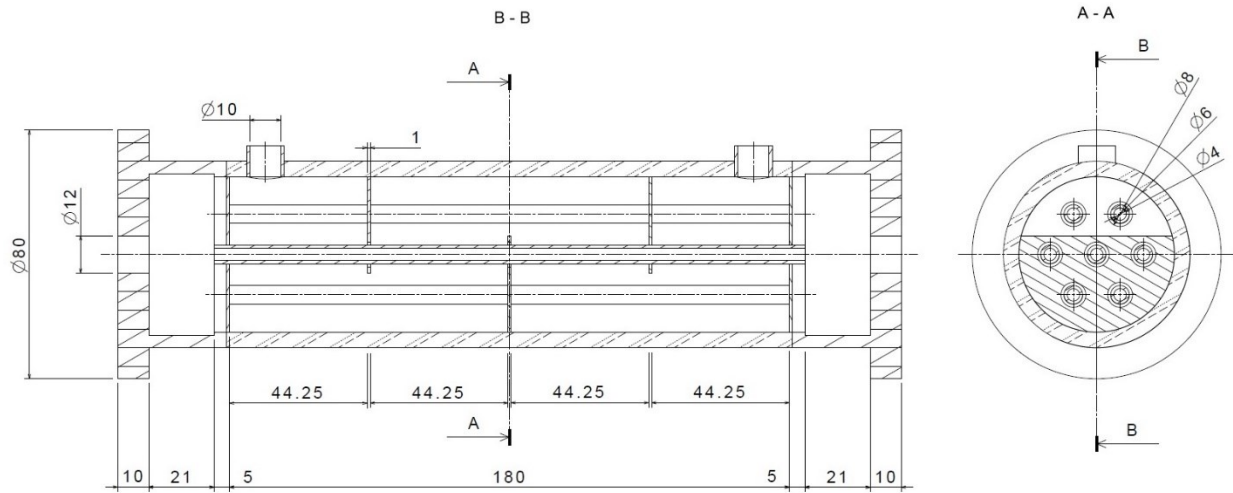


Figure 1. Heat exchanger cross-section with displayed dimensions.

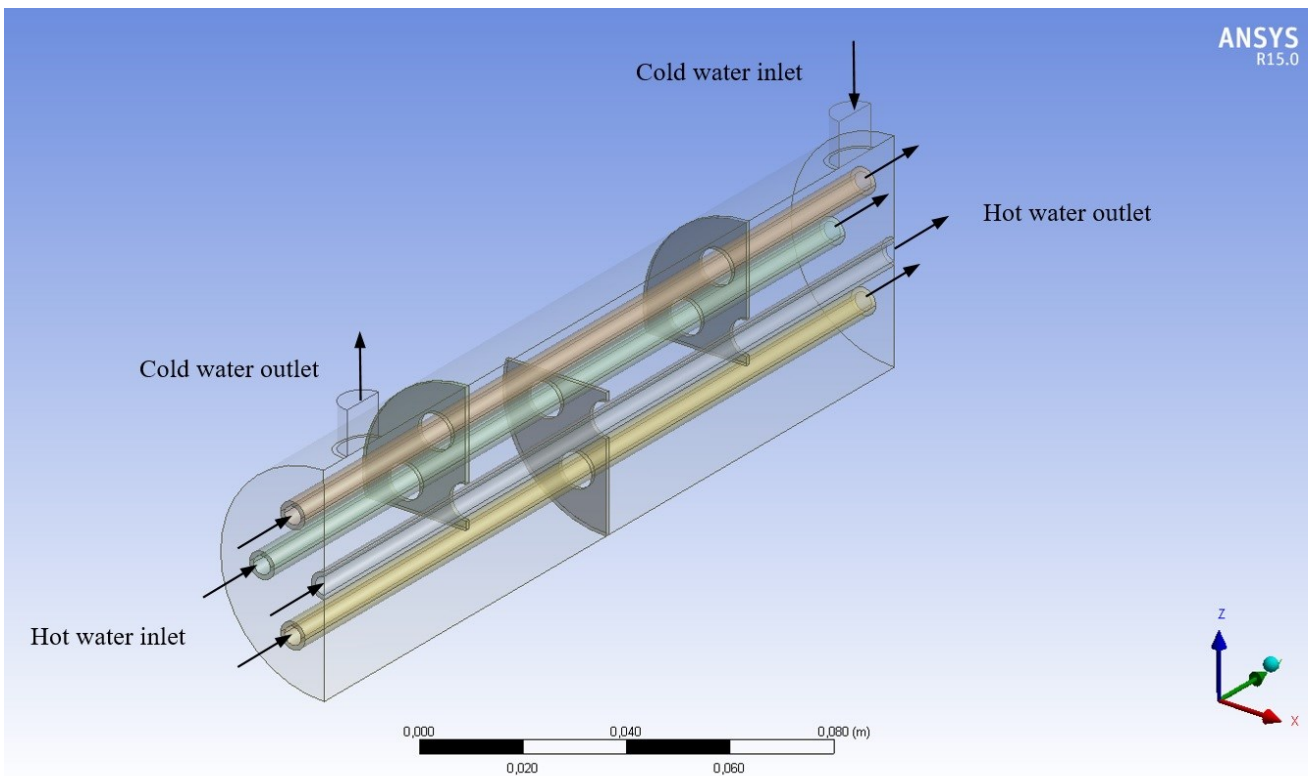


Figure 2. CAD model of the heat transfer domain.

The equations for laminar flow are as follows:

1. Hot water

$$\frac{\partial w_x}{\partial x} + \frac{\partial w_y}{\partial y} + \frac{\partial w_z}{\partial z} = 0 \quad (1)$$

$$\rho_{hw} \left(w_x \frac{\partial w_x}{\partial x} + w_y \frac{\partial w_x}{\partial y} + w_z \frac{\partial w_x}{\partial z} \right) = - \frac{\partial p}{\partial x} + \eta_{hw} \left(\frac{\partial^2 w_x}{\partial x^2} + \frac{\partial^2 w_x}{\partial y^2} + \frac{\partial^2 w_x}{\partial z^2} \right) \quad (2)$$

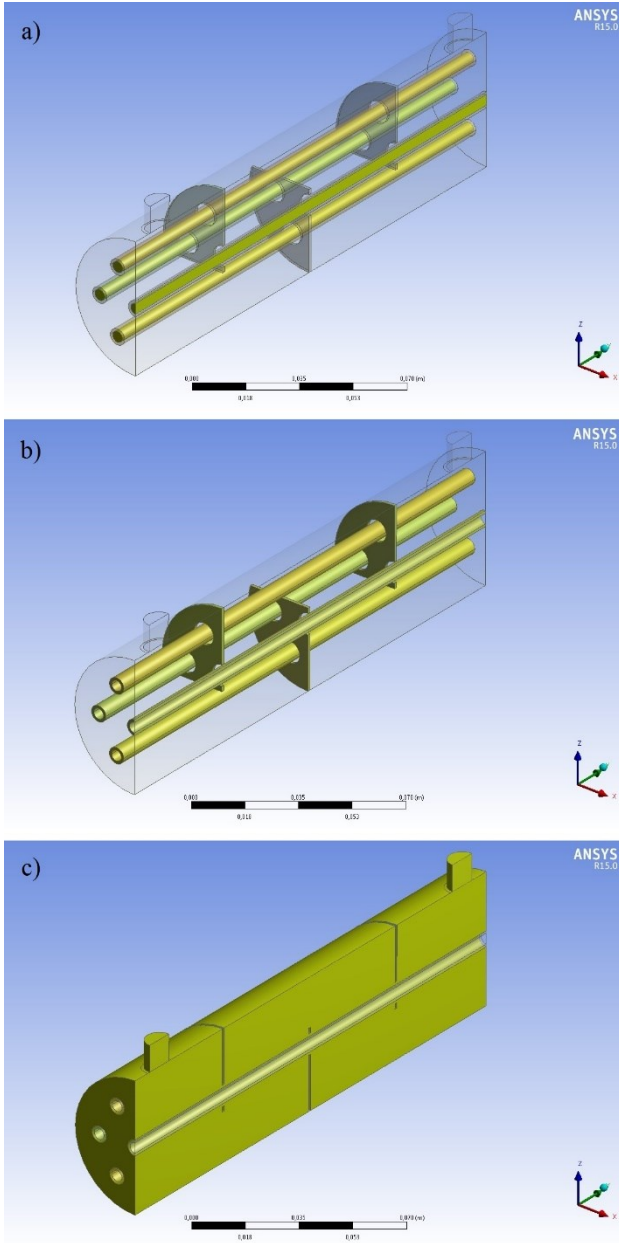


Figure 3. Calculation domain, (a) hot water subdomain, (b) wall subdomain, (c) cold water subdomain.

$$\rho_{hw} \left(w_x \frac{\partial w_y}{\partial x} + w_y \frac{\partial w_y}{\partial y} + w_z \frac{\partial w_y}{\partial z} \right) = -\frac{\partial p}{\partial y} + \eta_{hw} \left(\frac{\partial^2 w_y}{\partial x^2} + \frac{\partial^2 w_y}{\partial y^2} + \frac{\partial^2 w_y}{\partial z^2} \right) \quad (3)$$

$$\rho_{hw} \left(w_x \frac{\partial w_z}{\partial x} + w_y \frac{\partial w_z}{\partial y} + w_z \frac{\partial w_z}{\partial z} \right) = -\frac{\partial p}{\partial z} + \eta_{hw} \left(\frac{\partial^2 w_z}{\partial x^2} + \frac{\partial^2 w_z}{\partial y^2} + \frac{\partial^2 w_z}{\partial z^2} \right) \quad (4)$$

$$\rho_{hw} \left(w_x \frac{\partial T}{\partial x} + w_y \frac{\partial T}{\partial y} + w_z \frac{\partial T}{\partial z} \right) = \frac{\lambda_{hw}}{c_{hw}} \left(\frac{\partial^2 T}{\partial x^2} + \frac{\partial^2 T}{\partial y^2} + \frac{\partial^2 T}{\partial z^2} \right) \quad (5)$$

2. Wall

$$\frac{\partial^2 T}{\partial x^2} + \frac{\partial^2 T}{\partial y^2} + \frac{\partial^2 T}{\partial z^2} = 0 \quad (6)$$

3. Cold water

$$\frac{\partial w_x}{\partial x} + \frac{\partial w_y}{\partial y} + \frac{\partial w_z}{\partial z} = 0 \quad (7)$$

$$\rho_{cw} \left(w_x \frac{\partial w_x}{\partial x} + w_y \frac{\partial w_x}{\partial y} + w_z \frac{\partial w_x}{\partial z} \right) = -\frac{\partial p}{\partial x} + \eta_{cw} \left(\frac{\partial^2 w_x}{\partial x^2} + \frac{\partial^2 w_x}{\partial y^2} + \frac{\partial^2 w_x}{\partial z^2} \right) \quad (8)$$

$$\rho_{cw} \left(w_x \frac{\partial w_y}{\partial x} + w_y \frac{\partial w_y}{\partial y} + w_z \frac{\partial w_y}{\partial z} \right) = -\frac{\partial p}{\partial y} + \eta_{cw} \left(\frac{\partial^2 w_y}{\partial x^2} + \frac{\partial^2 w_y}{\partial y^2} + \frac{\partial^2 w_y}{\partial z^2} \right) \quad (9)$$

$$\rho_{cw} \left(w_x \frac{\partial w_z}{\partial x} + w_y \frac{\partial w_z}{\partial y} + w_z \frac{\partial w_z}{\partial z} \right) = -\frac{\partial p}{\partial z} + \eta_{cw} \left(\frac{\partial^2 w_z}{\partial x^2} + \frac{\partial^2 w_z}{\partial y^2} + \frac{\partial^2 w_z}{\partial z^2} \right) \quad (10)$$

$$\rho_{cw} \left(w_x \frac{\partial T}{\partial x} + w_y \frac{\partial T}{\partial y} + w_z \frac{\partial T}{\partial z} \right) = \frac{\lambda_{cw}}{c_{cw}} \left(\frac{\partial^2 T}{\partial x^2} + \frac{\partial^2 T}{\partial y^2} + \frac{\partial^2 T}{\partial z^2} \right) \quad (11)$$

2.3 Boundary conditions

Variables distribution within the domain is defined by boundary and initial conditions. Since the problem is steady state, only boundary conditions will apply.

The position of each boundary condition is highlighted green in Fig. 4.

Inlet boundary conditions are set at the entry point of each fluid at the model boundary. In this case, the values of velocity components and temperature are set. These values are based on the input parameters in each of the three experiments on the *TD360c* heat exchanger.

Outlet boundary conditions are set at the model outlet boundary perpendicular to the flow, where it is assumed that the flow is fully developed and no changes occur in flow direction, so the gradients of all variables (except pressure) are zero.

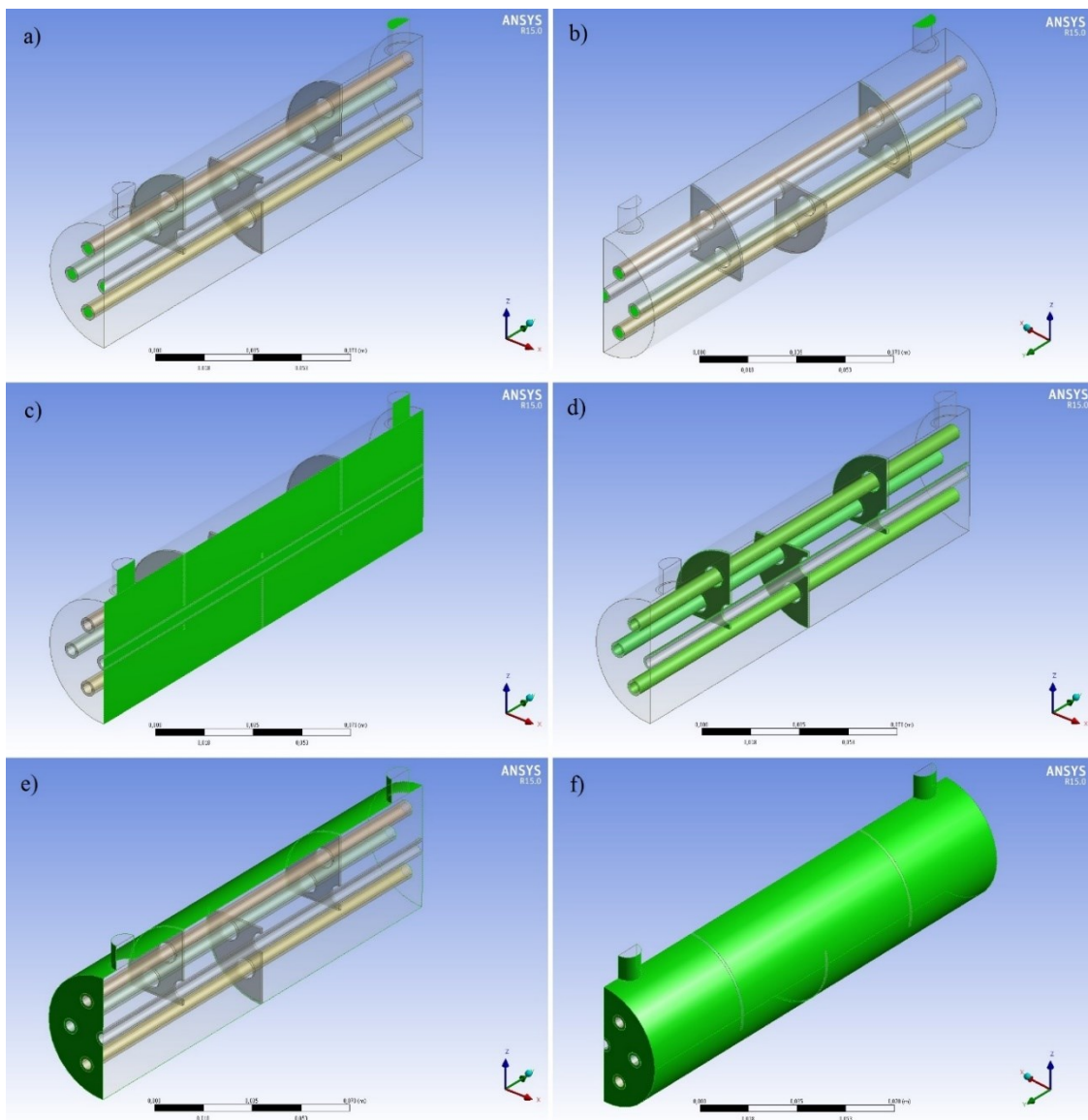


Figure 4. Boundary conditions marked in green, (a) inlet boundary condition, (b) outlet boundary condition, (c) symmetry boundary condition, (d) wall-water interface, (e) wall boundary condition (insulated), (f) wall boundary condition (insulated - rear).

For this problem, it means that gradients of fluid temperature and velocities are both zero:

$$\frac{\partial T}{\partial n} = 0 \quad (12)$$

$$\frac{\partial w_n}{\partial n} = 0 \quad (13)$$

Wall boundary conditions assume that the velocity components at the walls equal zero, $\vec{w} = 0$. It is also assumed that heat transfer within the boundary layer between the fluid and the wall occurs only by conduction:

$$\lambda_f \frac{\partial T}{\partial n} = \lambda_w \frac{\partial T}{\partial n} \quad (14)$$

In this particular instance, the thin layer of hot water in contact with the wall (inner tubes wall) delivers heat to the wall by conduction, the heat is conducted through the wall, and the cold water on the other side receives heat from the wall by conduction also. This boundary condition also applies to those surfaces of the baffles that are in contact with cold water.

Wall boundary conditions are also set at previously undefined surfaces of model edges, including surfaces of the baffles in contact with the shell. It is assumed that those surfaces are perfectly insulated and do not exchange heat with the environment.

$$\frac{\partial T}{\partial n} = 0 \quad (15)$$

Symmetry boundary condition is set along the longitudinal symmetry plane of the model. It states that the flow across the boundary equals zero, and that the scalar flow across the boundary is zero. For this problem, it means that the velocity component perpendicular to the symmetry line is equal to zero, as well as the gradients of temperatures and all other velocity components (ϕ being each of the variables in question):

$$w_n = 0 \quad (16)$$

$$\frac{\partial \phi}{\partial n} = 0 \quad (17)$$

3 Numerical solution

The problem was solved using the finite volume method, a numerical method based on the general conservation equation, described by Patankar [10]. Since velocity distribution throughout the model was unknown, an algorithm for its calculation was used. For pressure and velocity coupling, the *SIMPLE* (*Semi-Implicit Method for Pressure-Linked Equations*) algorithm was used. The numerical calculations were performed in *Ansys* (*Ansys Geometry, Ansys Mesh, Ansys Fluent*). A grid of 589922 cells was used. Mesh independency analysis has been performed. The used mesh has been selected as the most suitable with respect to accuracy of the solution and calculation duration. Fig. 5 shows the final mesh.

Convergence criteria were set for each of the conservation equations as follows:

- continuity: 10^{-3} ,
- momentum: 10^{-6} ,
- energy: 10^{-6} .

4 Experimental setup and validation

The experimental part of the research was done on the *TD360c*, an educational single flow shell-and-tube heat exchanger. Its parts, and the close-up of the device itself, are shown in Fig. 6. The entire system consists of the heat exchanger, control panel, a storage tank with heating capability, copper tubes which supply the fluids, and a pump which enables the circulation of the warmer fluid. On both ends of the exchanger, there are temperature sensors and flow meters, the measured values of which are displayed on the control panel for each fluid. Temperature is measured with thermocouples with an accuracy of ± 0.25 °C. The heat exchanger is so designed that the higher temperature fluid flows through the tubes, and the lower temperature one around them. In this case, both fluids are fed from a water supply and are at the same temperature. However, before reaching the heat exchanger, the fluid that is to flow through the tubes is heated to a desired temperature in the aforementioned tank, and afterwards pumped through the tubes. After passing the heat exchanger, it is refunded back to the tank and reheated. The temperature in the tank is defined on the control panel, the maximum value being 60 °C. The flows of

both fluids are controlled with the valves on the control panel, and, in this case, with the faucets. The lower temperature fluid connections can be switched so the heat exchanger can be used both in concurrent flow and countercurrent flow. Since concurrent flow is not as efficient as countercurrent flow, the latter is used.

All activities for this segment of the research were performed in the Laboratory for Thermal Measurements at the Faculty of Engineering, University of Rijeka. After filling the heat tank, desired temperature in the tank is set.

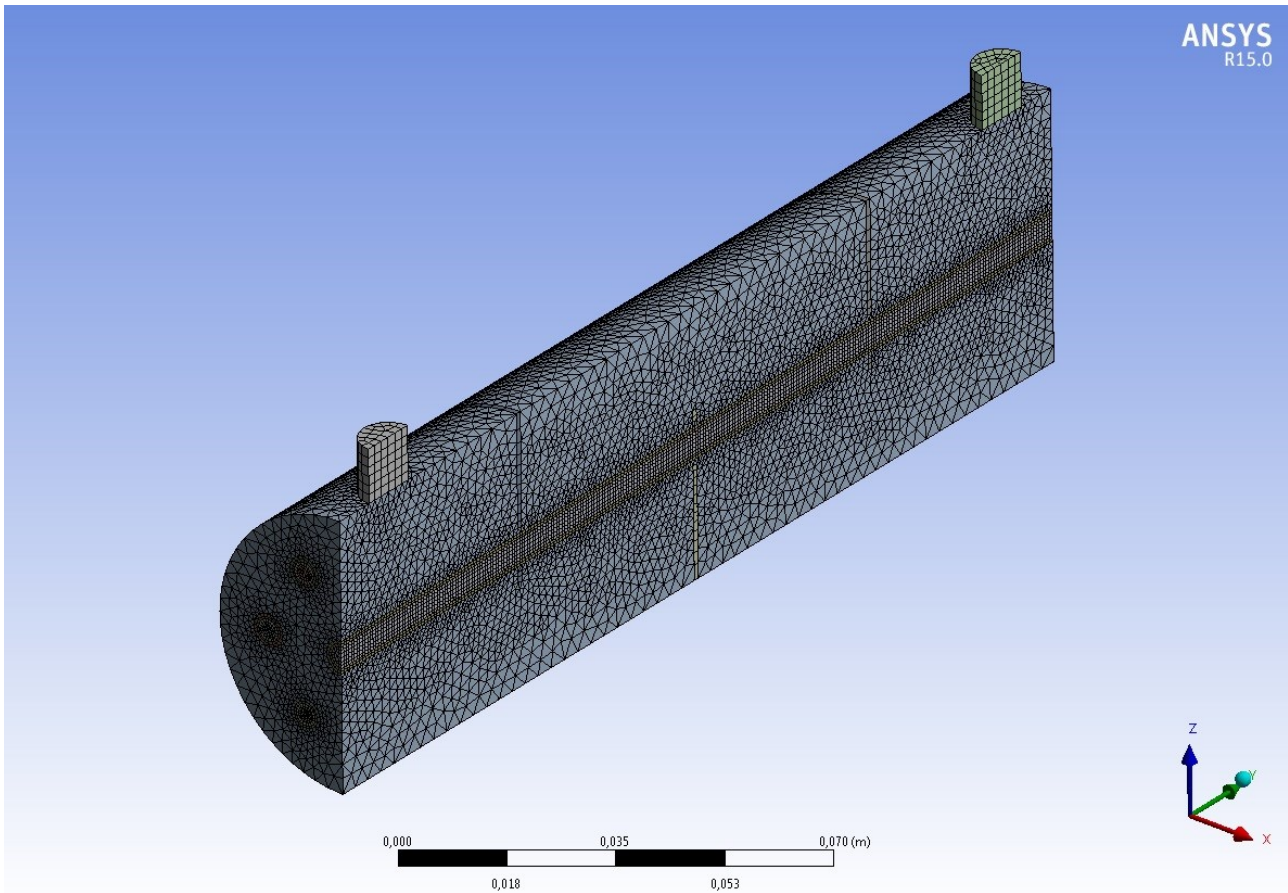


Figure 5. Meshed calculation domain.

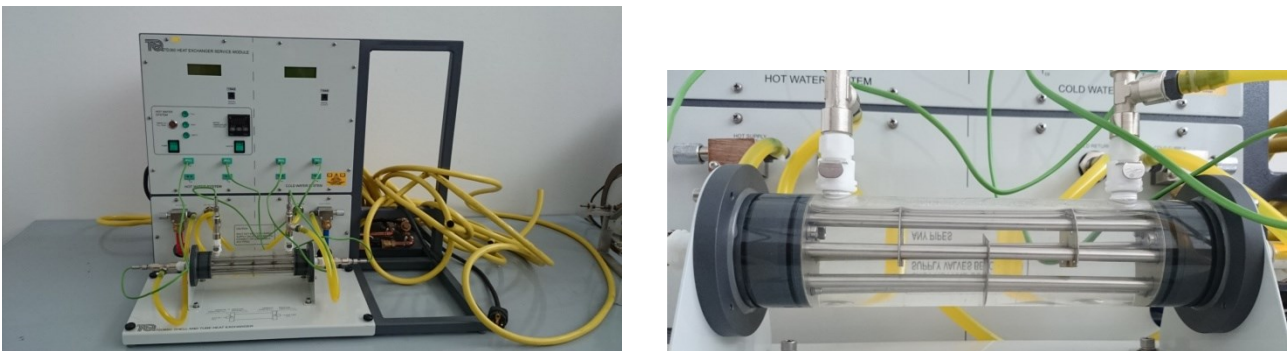


Figure 6. The TD360c heat exchanger system (left) and close-up of the device (right).

Cold water is fed from the water supply, so it enters the heat exchanger at the temperature that is in the water supply grid. There is a constant flow of both fluids through the heat exchanger, and it is regulated on the faucet or small valves at their entrance to the device.

During the first experiment, after about ten minutes of fluctuation, the heat exchange got steady, i.e. there were no changes in each of the temperature values.

For additional validity check of numerical results, a heat fluxes balance between hot and cold water has been calculated:

$$\begin{aligned} \dot{V}_{hw} \cdot \rho_{hw} \cdot c_{hw} \cdot (t'_{hw} - t''_{hw}) = \\ \dot{V}_{cw} \cdot \rho_{cw} \cdot c_{cw} \cdot (t''_{cw} - t'_{cw}) \end{aligned} \quad (18)$$

The second and third experiments differ from the first one in terms of temperature (lower than the first) and volume flow (twice as big as the first), respectively. Table 1 shows inlet parameters (temperature and flow), outlet temperatures for both hot and cold water for all three experiments, and heat fluxes on both sides.

5 Numerical results

Numerical calculations have been performed for three different cases in total, input parameters of which are displayed in Table 1. These parameters match the conditions set in the three experiments on the heat exchanger *TD360c*.

Fig. 7 displays the temperature distribution within the heat exchanger for the first set of input parameters. A

decrease in temperature is clearly visible in the central tube section. Consequently, an increase in cold water temperature along the shell is shown, as well as the influence of the baffles, which increase heat transfer by prolonging the passage of cold water, as well as turbulence.

Fig. 8 displays velocity vectors and Fig. 9 the close-ups on the entry and exit points for each fluid. It is visible that both fluids enter the heat exchanger with a uniformed velocity profile, and once the flow has progressed, their profile becomes less uniformed, i.e. the flow gets more developed. It is also visible that due to the no-slip condition, velocity is highest at the tubes' center and lowest as it approaches the tubes' wall.

In order to preserve continuity, there needs to be an increase at the center to compensate for the drop at the edge.

Calculations results will also serve in setting up heat fluxes balance between the hot and cold water. It will, along with outlet fluid temperatures, serve as an additional validity check for the model.

The heat flux given away by hot water must be equal to the heat flux received by cold water:

$$\dot{Q}_1 = \dot{Q}_2 \quad (19)$$

For each fluid, heat fluxes calculated from the data acquired in numerical investigation are represented in Table 2.

Table 2 shows variations in outlet temperatures for both fluids—due to varying inlet conditions in each case.

Table 1. Experimentally obtained outlet temperatures and heat fluxes for different water inlet parameters

Case	Hot water				Cold water			
	\dot{V}_{hw} [m ³ /s]	t'_{hw} [°C]	t''_{hw} [°C]	\dot{Q}_1 [W]	\dot{V}_{cw} [m ³ /s]	t'_{cw} [°C]	t''_{cw} [°C]	\dot{Q}_2 [W]
1	$8.5 \cdot 10^{-6}$	56.4	49.3	249.1	$7.5 \cdot 10^{-6}$	26.9	35	252.7
2	$8.33 \cdot 10^{-6}$	43.3	39.6	128.3	$8.33 \cdot 10^{-6}$	26.4	30	124.9
3	$1.67 \cdot 10^{-5}$	57.9	52.3	384.8	$1.7 \cdot 10^{-5}$	26.5	32.3	410.4

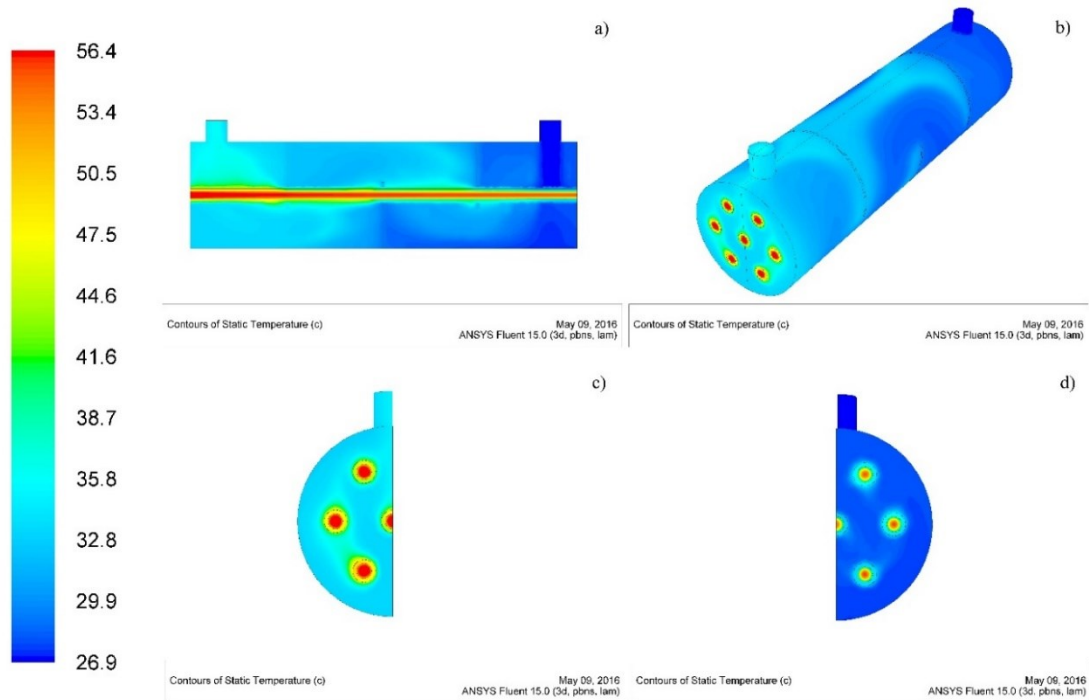


Figure 6. Temperature distribution within the heat exchanger for $t_{hw} = 56.4 \text{ }^\circ\text{C}$, $w_{hw} = 0.1 \text{ m/s}$, $t_{cw} = 26.9 \text{ }^\circ\text{C}$: $w_{cw} = 0.095 \text{ m/s}$: (a) front view, (b) isometric view, (c) hot water inlet section, (d) hot water outlet section.

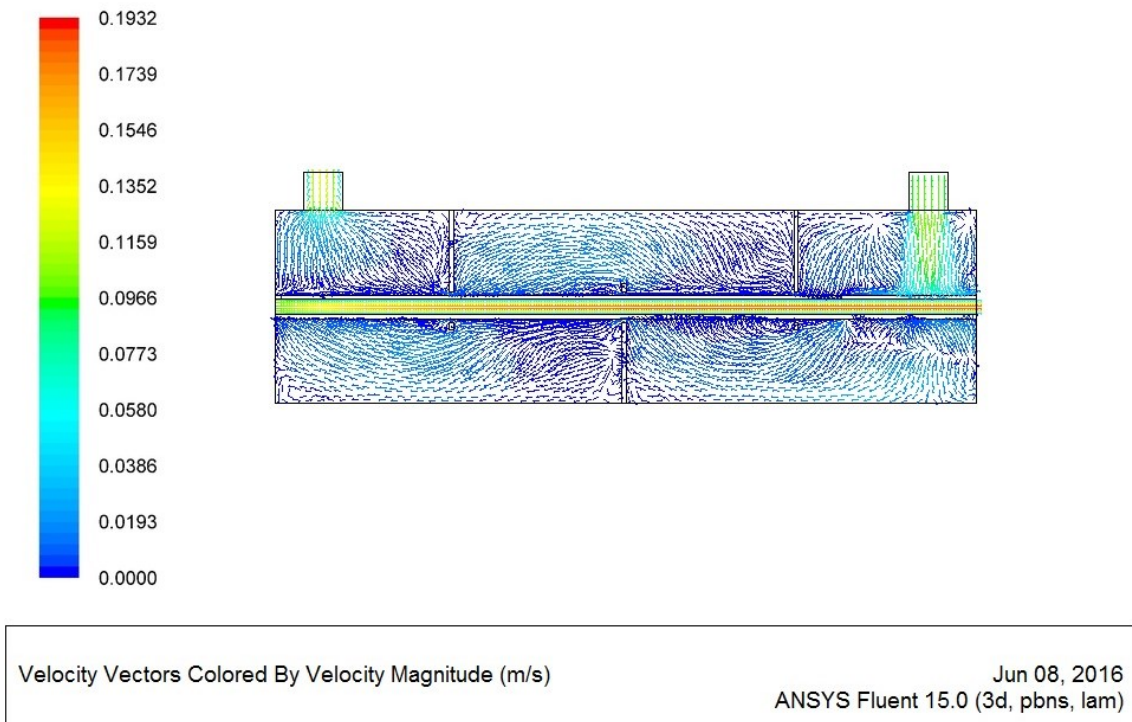


Figure 7. Velocity vectors in the symmetry plane for $t_{hw} = 56.4 \text{ }^\circ\text{C}$, $w_{hw} = 0.1 \text{ m/s}$, $t_{cw} = 26.9 \text{ }^\circ\text{C}$: $w_{cw} = 0.095 \text{ m/s}$ in the symmetry plane (vector color denotes velocity intensity).

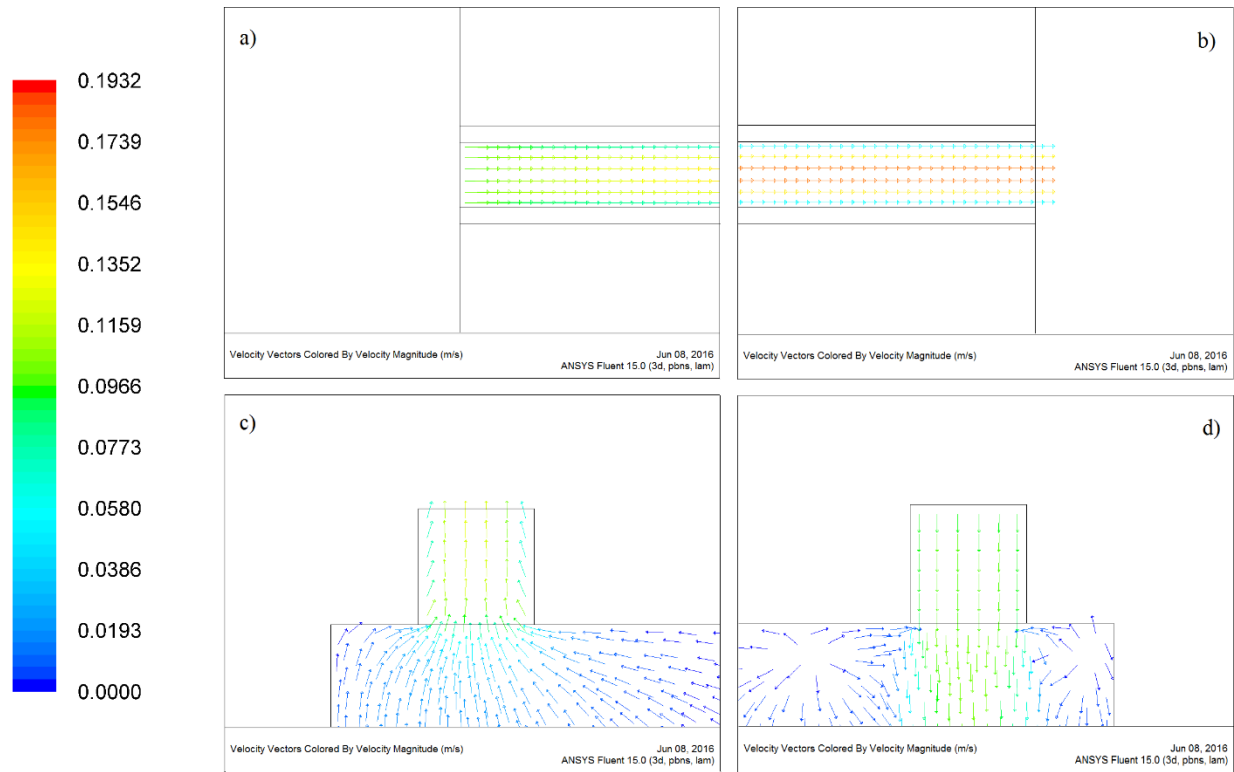


Figure 8. Close-ups of velocity vectors: (a) hot water inlet, (b) hot water outlet, (c) cold water outlet, (d) cold water inlet (vector color denotes velocity intensity).

Table 2. Numerically obtained outlet temperatures and heat fluxes on both sides for different water inlet temperatures

Case	Hot water		Cold water	
	t''_{hw} [°C]	\dot{Q}_1 [W]	t''_{cw} [°C]	\dot{Q}_2 [W]
1	49.6	237.5	34.6	238.9
2	39.3	139.1	30.5	140.1
3	52.7	363.4	31.7	367.4

In the case 2; where the inlet temperature of hot water is lower than the first one, outlet temperatures vary less than in the first experiment. That is to be expected, considering the decrease in inlet temperature difference of both fluids, which results in a less intense heat transfer. A direct result of

smaller inlet temperature difference is a decrease in the heat flux values.

In the case 3; where hot and cold water volume flows are approximately twice the value of the first, cold water outlet temperature is lower in comparison with the case 1. Providing the flows of both hot and cold water have doubled, the hot water does not cool, and the cold water does not warm to the extent as they did in the case 1. The heat flux is the highest in this case, the reason being the flow increase with respect to the first case. After having made three numerical investigations and three experiments with different inlet parameters, the results of both methods need to be compared in order to assess the model's validity. This comparison is presented in Table 3, which shows outlet temperatures of hot and cold water, as well as both heat fluxes. The table shows a very good match between outlet temperatures of both fluids and between heat fluxes acquired by numerical calculation and experimental data in all three cases considered. It can be concluded that this model faithfully represents the phenomenon of heat transfer in the small size TD360c shell-and-tube heat exchanger.

Table 3. Comparison of outlet temperatures and heat fluxes on both sides for numerical and experimental investigation

Case	Numerical model				Experimental results			
	t''_{hw} [°C]	t''_{cw} [°C]	\dot{Q}_1 [W]	\dot{Q}_2 [W]	t''_{hw} [°C]	t''_{cw} [°C]	\dot{Q}_1 [W]	\dot{Q}_2 [W]
1	49.6	34.6	237.5	238.9	49.3	35	249.1	252.7
2	39.3	30.5	139.1	140.1	39.6	30	128.3	124.9
3	52.7	31.7	363.4	367.4	52.3	32.3	384.8	410.4

6 Conclusion

The purpose of this research was both to design a numerical model of an educational shell-and-tube water-water heat exchanger (the TecQuipment's *TD360c*) and, using the data acquired in experimental research, to question its validity. It was done by performing three experiments with different inlet parameters, which were later used in the numerical calculations. The model was solved with the finite volume method, using the SIMPLE algorithm, for laminar flow and steady state heat transfer. Numerical analysis was performed using *Ansys (Geometry, Mesh, Fluent)* software.

By comparing the results acquired by both numerical modelling and experimental investigation, a validity assessment of the model was determined.

Outlet temperatures of both hot and cold water, as well as heat fluxes, calculated numerically and measured experimentally in all three cases show a satisfactory match, which points to a conclusion that the model accurately describes the heat transfer problem within the educational *TD360c* heat exchanger. The developed model can be used in further studies as a basis for creating other similar models of fluid flow and heat transfer in shell and tube heat exchangers.

Nomenclature

c	Specific heat capacity, J/kgK
F	Area of heat transfer, m ²
n	Normal
p	Pressure, Pa
\dot{Q}	Heat flux, W
\dot{q}	Heat flux density, W/m ²

T	Temperature, K
t'	Water inlet temperature, °C
t''	Water outlet temperature, °C
\dot{V}	Volume flow, m ³ /s
w	Velocity, m/s
x, y, z	Coordinates, m

Greek symbols

η	Dynamic viscosity, Pa·s
λ	Thermal conductivity, W/mK
ρ	Density, kg/m ³
ϕ	Physical property, various

Subscripts

cw	Cold water
f	Fluid
hw	Hot water
n	Normal
w	Wall

References

- [1] Jadhav, A.D., Koli, T.A.: *CFD Analysis of Shell and Tube Heat Exchanger to Study the Effect of Baffle Cut on the Pressure Drop*, International Journal of Research in Aeronautical and Mechanical Engineering, 2 (2014), 7, 1-7.
- [2] Arjun K.S., Gopu K.B.: *Design of Shell and Tube Heat Exchanger Using Computational Fluid Dynamics Tools*, Research Journal of Engineering Sciences, 3 (2014), 7, 8-16.
- [3] Wen, J., Yang, H., Wang, S., Xue, Y., Tong, X.: *Experimental investigation on performance comparison for shell-and-tube heat exchangers*

- with different baffles, *International Journal of Heat and Mass Transfer* 84 (2015), 990-997.
- [4] You, Y., Chen, Y., Xie, M., Luo, X., Jiao, L., Huang, S.: *Numerical simulation and performance improvement for a small size shell-and-tube heat exchanger with trefoil-hole baffles*, *Applied Thermal Engineering*, 89 (2015), 220-228.
- [5] Pal, E., Kumar, I., Joshi, J.B., Maheshwari, N.K.: *CFD simulations of shell-side flow in a shell-and-tube type heat exchanger with and without baffles*, *Chemical Engineering Science*, 143 (2016), 314-340.
- [6] Kim, W-K, Aicher, T.: *Experimental investigation of heat transfer in shell-and-tube heat exchangers without baffles*, *Korean J. of Chem. Eng.*, 14 (1997), 2, 93-100.
- [7] Vukić, M. Vučković, G., Živković, P., Stevanović, Ž., Tomić, M.: *3D Numerical Simulations of the Thermal Processes in the Shell and Tube Heat Exchanger*, *Facta Universitatis, Series: Mechanical Engineering*, 11 (2013), 2, 169-180.
- [8] Yang, J., Liu, W.: *Numerical investigation on a novel shell-and-tube heat exchanger with plate baffles and experimental validation*, *Energy Conversion and Management* 101 (2015), 689–696.
- [9] Yang, J., Ma, L. Bock, J., Jacobi, A.M., Liu, W.: *A comparison of four numerical modeling approaches for enhanced shell-and-tube heat exchangers with experimental validation*, *Applied Thermal Engineering*, 65 (2014), 1-2, 369-383
- [10] S.V. Patankar: *Numerical Heat Transfer and Fluid Flow*, Hemisphere Publishing Corporation, Taylor & Francis Group, New York, 1980.